PERGAMON

International Journal of Solids and Structures 36 (1999) 3407–3425

INTERNATIONAL JOURNAL OF SOLIDS and STRUCTURES

Ductile fracture of materials with high void volume fraction

K. S. Zhang[a], J. B. Bai[b,*], D. François[b]

[a] *Northwestern Polytechnical University, 710072, Xi'an, P.R. China*
[b] *Lab. MSS/MAT, CNRS URA 850, Ecole Centrale de Paris, 92295 Châtenay Malabry Cedex, France*

Received 9 July 1997; in revised form 23 April 1998

Abstract

In the present paper, axisymmetric cell models containing one or two voids and a three-dimensional cell model containing two voids have been used to investigate void size and spacing effect on the ductile fracture in materials with high initial void volume fraction. They are performed for round smooth and round notched specimens under uniaxial tension. The example material used for comparison is a nodular cast iron material GGG-40 with initial void volume fraction of 7.7%. The parameters considered in this paper are void size and shape for axisymmetric cell models containing a single void, and void distribution pattern for axisymmetric and 3D cell models containing two voids of different sizes. The results obtained from these cell models by using FEM calculations are compared with the Gurson model, the Gurson–Tvergaard–Needleman model, the Rice–Tracey model and the modified Rice–Tracey model. It can be stated that the influence of void size and void spacing on the growth in volume of voids is very large, and it is dependent on the distribution of voids. Using non-uniform void distribution, the results of axisymmetric cell models can explain how a void can grow in an unstable state under very low stress triaxiality at very small strain as observed in experiments. Calculations using cell models containing two voids give very different results about the stable and unstable growth of voids which are strongly dependent on the configuration of cell model.

Keywords: Ductile fracture; Void size and spacing; Porous material; Cell model containing two voids; 3D FEM calculation

1. Introduction

The damage and fracture of ductile metal materials under tension load can be attributed to the nucleation, growth and coalescence of voids. In early research, Rice and Tracey (1969) suggested the R-T model to describe the growth of a spherical void, in a infinite perfectly plastic solid, subject to a remote uniform stress and strain field. On the basis of the results of the R-T model, Gurson further considered a spherical void contained cell with finite volume and suggested a plastic potential function for porous materials (Gurson, 1977). By using this function, Gurson's consti-

* Corresponding author. Fax: 00 33 1 41 13 14 60; E-mail: baijinbo@mssmat.ecp.fr

0020–7683/99/$ - see front matter
PII: S0020–7683(98)00157–7

tutive equation can be derived and, further, the void nucleation, growth and coalescence can all be taken into account. Since this model has the advantage of simulating the damage and fracture taking place in ductile materials, it has been studied by many researchers. The most important improvement on the Gurson model was made by Tvergaard and Needleman. Applying cell models, Tvergaard studied the plastic flow localization (Tvergaard, 1982), and later by using these results Tvergaard and Needleman (1984) suggested a further modification to describe the sharp drop of stress in materials after the coalescence of voids. Their constitutive relations referred to as the GTN model have been adopted by many researchers to analyze and predict the ductile damage and fracture in metal materials.

Since these models were proposed under very ideal conditions, and some coefficients in the Gurson and GTN models were not of clear physical meaning, both are difficult to use for actual engineering materials. There is often a significant discrepancy between the modeling results and the experimental data. To improve these models further, the study of the ferric nodular cast iron material has been paid great attention, not only due to its microstructure, very close to the ideal porous material with spherical void, but also for its wide industry application. The previous results showed that the Gurson model or GTN model, studied by using a cell model with identical void size and spacing, gives largely overestimated fracture strain compared to the experimental data of a round smooth bar under uniaxial tension (Brocks et al., 1996; Kuna et al., 1996; Dong et al., 1996).

Considering that the microscopic distributions of the size and the spacing of voids in different places in a real material are very different, the assumption of uniform void size and spacing may ignore the effect of void interaction and of different void sizes on the material damage. In porous materials, the non-uniformity of void size and spacing implies that the resistance to fracture of the material is also non-uniform in the void size scale or in the void spacing scale. That the local properties of resistance to fracture in a material should be different implies that the material of non-uniform microstructures is more easily damaged and fractured compared to that with microstructure considered to be average.

In the present paper, in order to investigate the influence of non-uniform factors on the fracture of material, the different axisymmetric cell models containing one void or two voids with different geometries is applied so that the effect of void size and spacing and void interaction may be considered. Furthermore, the 3D cell model containing two voids of different sizes are employed to evaluate the competition of void growth and the effect of void distribution on it. The loading condition is for a round smooth specimen and a round notched specimen made of a nodular cast iron material GGG-40 under tension with graphite volume fraction 7.7%. The results obtained from cell models by using large elastic plastic FEM calculations are also compared with the Gurson model (1969), the GTN model (Tvergaard and Needleman, 1984), the RT model (Rice and Tracey, 1969) and the modified RT model (Huang, 1991).

2. Example material and specimens

The material investigated in the present paper is nodular cast iron GGG-40. This material has a rather high initial volume fraction of graphite (7.7%), and the shape of graphite inclusions can be approximated as spherical or ellipsoidal particles. Because graphite inclusions are very soft

Table 1
The chemical compositions of GGG-40

C	Si	Mn	S	P	Mg	Cu	Ni	Cr	Fer
3.35	2.25	0.30	0.006	0.025	0.039	0.06	0.04	0.02	93.9

Table 2
Main mechanical properties of GGG-40

E (GPa)	v	$\sigma_{0.2}$(MPa)	σ_b(MPa)	Ψ (%)
187	0.28	260	393	22.9

compared to the matrix, the material can be considered to be porous medium containing voids of the same size as the graphite inclusions. The chemical composition of the material is shown in Table 1. Its parameters of mechanical properties are shown in Table 2. The true stress-logarithmic strain curves of the material GGG-40 and its matrix material are shown in Fig. 1. The Young's modulus, Poisson's ratio and yield strength of the matrix of GGG-40 are respectively 210 GPa, 0.3 and 295 MPa. The smooth round tensile specimen is 5 mm in diameter with gauge length 25 mm, and the notched round tensile specimen is 5 mm in diameter with 4 mm notch radius (AE4).

3. Cell model

The mechanical behavior of porous solids can be simulated by cell model calculations. Koplik and Needleman (1988), Brocks et al. (1995) adopted the axisymmetrical cylindrical unit cell with

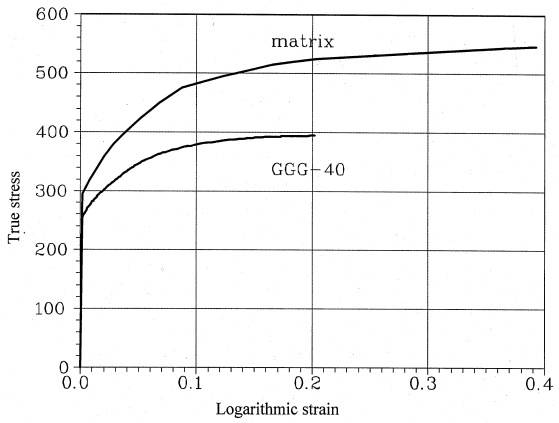

Fig. 1. True stress–logarithmic strain curves of GGG-40 and its matrix.

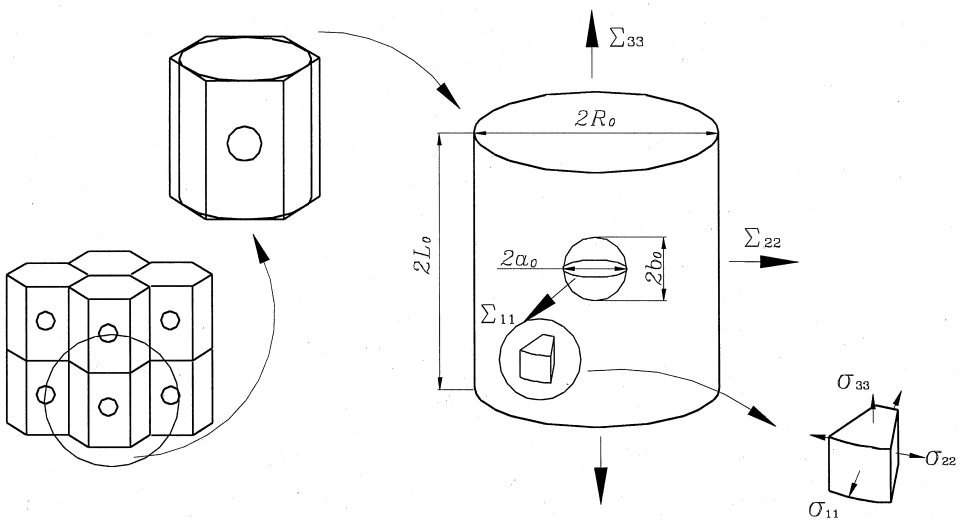

Fig. 2. The one void contained cylindrical cell.

one void in it to study void growth under different given stress triaxialities, in order to examine Gurson mode, and, further to fit the parameters of the GTN model. Tvergaard used the cell model with two voids to investigate the plastic flow localization and the interaction between two voids of different sizes (Tvergaard, 1996). The 3D cell with one void has been used to analyze the void growth in different stress states by Worswick and Pick (1990), Kuna and Sun (1996) and Zhang and Zheng (1997). Because the cell model can describe the relations between the macroscopic mechanical behavior and the microstructure of a material, it has been used by many researchers to investigate various problems.

In the present paper, the cylindrical unit cell with one or two voids is used. To consider the effect of non-uniform void size and spacing, besides changing the geometric parameters of the cell model with one void, a cylindrical cell and a three-dimensional brick cell containing two voids of different size are also considered.

Figure 2 shows the geometry of a cylindrical cell containing one void. This cell is used when the material is assumed to be a periodic array of identical voids. The initial void volume fraction can be written as:

$$f_0 = \frac{2a_0^2 b_0}{3R_0^2 L_0} \tag{1}$$

Meanwhile the void spacing parameter L_{r0} and void shape parameter S_{r0} are defined as:

$$L_{r0} = \frac{L_0}{R_0}; \quad S_{r0} = \frac{a_0}{b_0}$$

The hole in Fig. 2 is an ellipsoidal sphere. The current void volume fraction f is defined as:

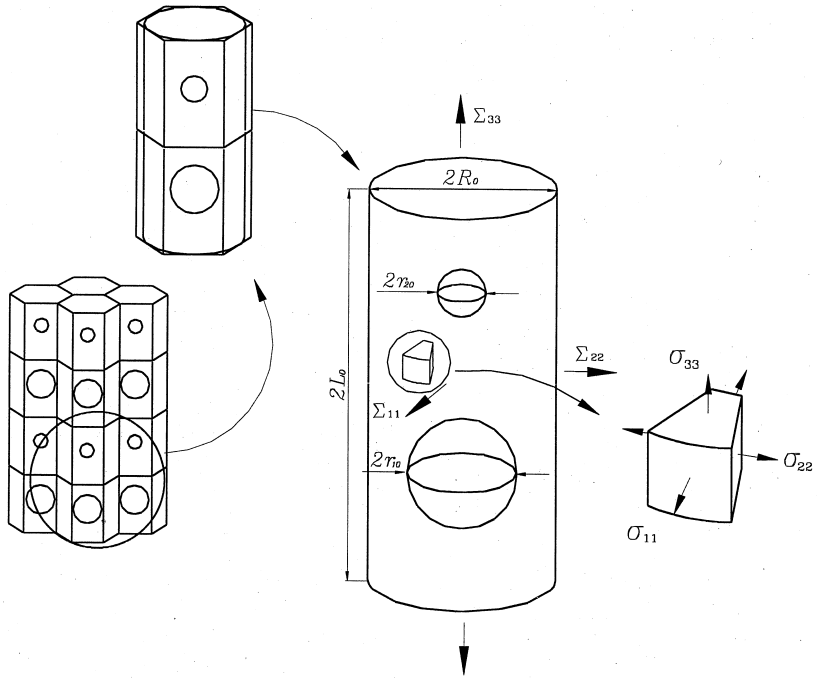

Fig. 3. The geometry of two voids contained cylindrical cell.

$$f = \frac{V_{\text{void}}}{V} \tag{2}$$

V_{void} is the volume of the void in the cell, and V is the total volume of the cell. The current void volume fraction f can be calculated by using the nodal displacements obtained from FEM calculation.

Figure 3 shows the geometry of a cylindrical cell containing two voids. Using this cell means the model material contains a periodic array of two voids with different sizes. The initial f can be defined as:

$$f_0 = f_{10} + f_{20}; \quad f_{10} = \frac{2r_{10}^3}{3R_0^2 L_0}; \quad f_{20} = \frac{2r_{20}^3}{3R_0^2 L_0} \tag{3}$$

It should be pointed out that the cell with one void, as in Fig. 2, and the cell with two voids, as in Fig. 3, do not represent the true configuration of actual materials. In the actual material, the distribution of voids is random, and can not be calculated by current methods. Although a simple cell can not describe the real case, the voids with random distributions, it is possible to show the effect of void size and spacing that can be found in some areas in an actual material.

The current f can be defined as the sum of two parts:

$$f = f_1 + f_2; \quad f_1 = \frac{V_{\text{void1}}}{V}; \quad f_2 = \frac{V_{\text{void2}}}{V} \tag{4}$$

For the above two cells the principal strains and the effective strain can be given by:

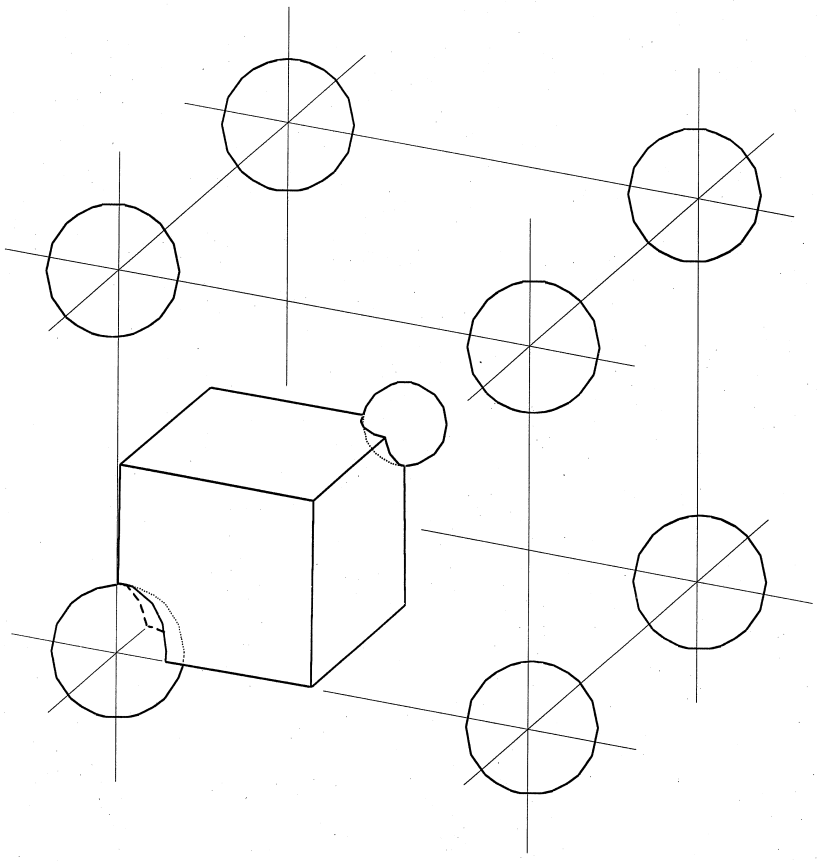

Fig. 4. A 3D cell containing two spherical voids with different size drawn from periodic array of voids.

$$E_1 = E_2 = \ln\left(\frac{R}{R_0}\right); \quad E_3 = \ln\left(\frac{L}{L_0}\right); \quad E_e = \frac{2}{3}\int(\dot{E}_3 - \dot{E}_1)\,dt \tag{5}$$

Tvergaard also analyzed a cell (Tvergaard, 1996) containing two voids, but with different boundary conditions than those in the present paper. They correspond to two different periodic arrays of voids. In order to consider the effect of different arrays of voids, a three-dimensional two void cell with different void sizes is used in the present paper (cf Fig. 4). The periodic array of voids represented by this cell is very similar to that in Tvergaard (1996), where the conditions are simplified and an axisymmetric cell model was employed and the loading direction was different from the present.

The initial f in this cell can be written as:

$$f_0 = f_{10} + f_{20}; \quad f_{10} = \frac{\pi}{6}\frac{r_{10}^3}{L_{10}L_{20}L_{30}}; \quad f_{20} = \frac{\pi}{6}\frac{r_{20}^3}{L_{10}L_{20}L_{30}} \tag{6}$$

The current volume fraction of voids can also be described by eqn (4). The principal strains and the effective strain, respectively, are given by:

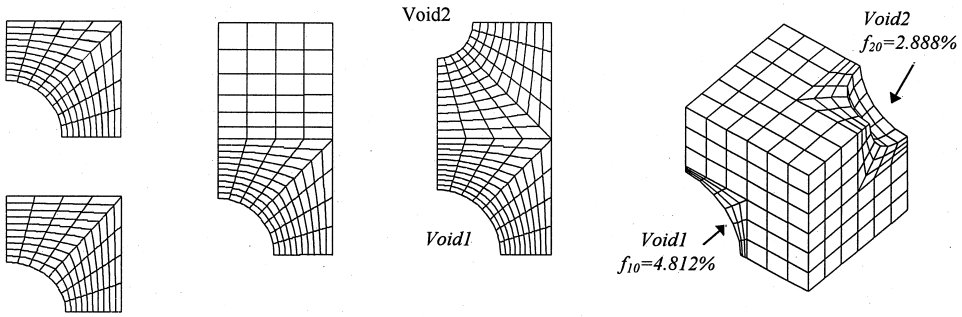

Fig. 5. Different meshes of cell models.

$$E_1 = \ln\left(\frac{L_1}{L_{10}}\right); \quad E_2 = \ln\left(\frac{L_2}{L_{20}}\right); \quad E_3 = \ln\left(\frac{L_3}{L_{30}}\right)$$

$$E_e = \frac{\sqrt{2}}{3}\int[(\dot{E}_1-\dot{E}_2)^2+(\dot{E}_2-\dot{E}_3)^2+(\dot{E}_3-\dot{E}_1)^2]^{1/2}\,dt \tag{7}$$

The corresponding true principal stress for the above axisymmetrical cell models and 3D cell models, Σ_1, Σ_2, Σ_3 are the average reaction forces at the cell boundaries per momentary areas.
In the present paper, the capital letters, Σ_{ij}, E_{ij}, denote the quantities on cell length scale and small letters, σ_{if}, ε_{ij}, quantities on a 'microscopic' scale, respectively.

The effective stress, hydrostatic stress and triaxiality parameter are defined as:

$$\Sigma_e = \frac{1}{\sqrt{2}}\sqrt{(\Sigma_1-\Sigma_2)^2+(\Sigma_2-\Sigma_3)^2+(\Sigma_3-\Sigma_1)^2}; \quad \Sigma_h = \tfrac{1}{3}(\Sigma_1+\Sigma_2+\Sigma_3)$$

$$T = \frac{\Sigma_h}{\Sigma_e} \tag{8}$$

The different types of finite element meshes for different cell models are shown in Fig. 5. In axisymmetric analysis the eight-node element is used, and the twenty-node element is used in 3D analysis. The large strain finite element calculations are performed using a special program for ductile fracture analysis.

4. Results and discussion

The loads are controlled by a subroutine which is developed on the basis introduced in Brocks et al. (1995). Because the fractures were initiated in the neck centers of both smooth and notched bars, the triaxiality control was set according to the curves of stress triaxiality vs plastic effective

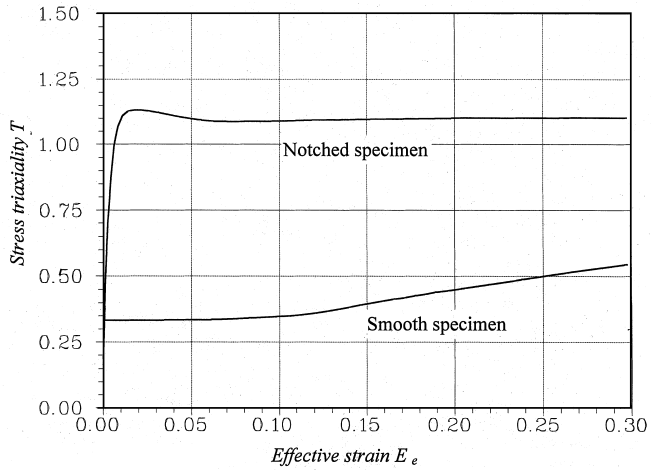

Fig. 6. Stress triaxiality with effective strain at the neck centre of specimens.

strain in the centers of these specimens under tension. Figure 6 shows the curves of triaxiality parameter T vs plastic effective strain E_e^p in neck centers of two types of specimens. Figures 7a) and b) show the relationships of void relative growth vs effective strain, for the neck centers of round smooth and notched bars by using different cells in which the cell parameters are $L_{r0} = 1$ and $S_{r0} = 1$, but the initial f_0 are respectively 3.85, 7.7, 11.55 and 15.4%. It can be found, from this figure, that the relative growth of voids for different f are nearly the same at the beginning of loading. The cell with smaller value of f grows slightly faster than the one with larger value of f. With the increase of effective strain, the tendency is slowly changed, and the cell with larger value of f will enter the faster growing stage earlier than the one with smaller value of f. This means that the relative void growth in terms of volume fraction increase are almost the same for the cells with identical spacing but with different initial f for stable void growth stage. However, the growth law is different once the larger void enters into unstable growth.

For comparison, the Gurson model, the GTN model, the RT model and the modified RT model (Huang, 1991) are also considered here. For the Gurson model and the GTN model, the curves of relative void growth vs plastic effective strain can be obtained from integration by using Gurson or GTN constitutive equations. Gurson's plastic potential function, which has been modified by Tvergaard and Needleman (1984), can be written as:

$$\Phi = \frac{\Sigma_e^2}{\sigma_M^2} + 2q_1 f^* \cos h\left(q_2 \frac{3\Sigma_h}{2\sigma_M}\right) - 1 - q_3 f^{*2} = 0 \tag{9}$$

where σ_M is the flow stress of the matrix material, Σ_e and Σ_h are the effective stress and hydrostatic stress of porous materials. The parameters q_i were introduced by Tvergaard and Needleman, and in many applications q_2 and q_3 were set to $q_2 = 1$, $q_3 = q_1^2$. The value of q_1 varies from 1 to 1.5. Additionally, the damage variable, f^*, is introduced by

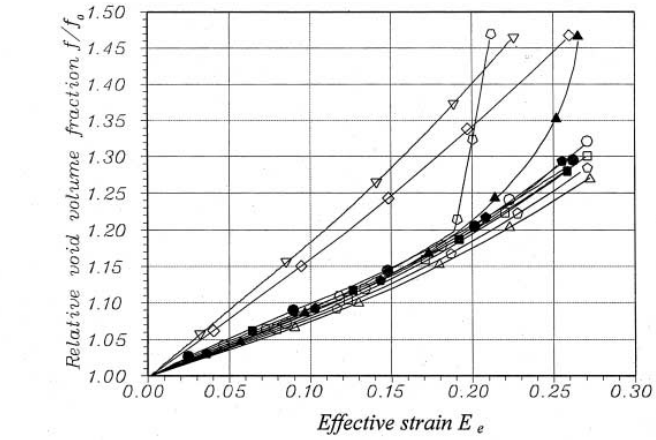

a) in the neck center of round bar

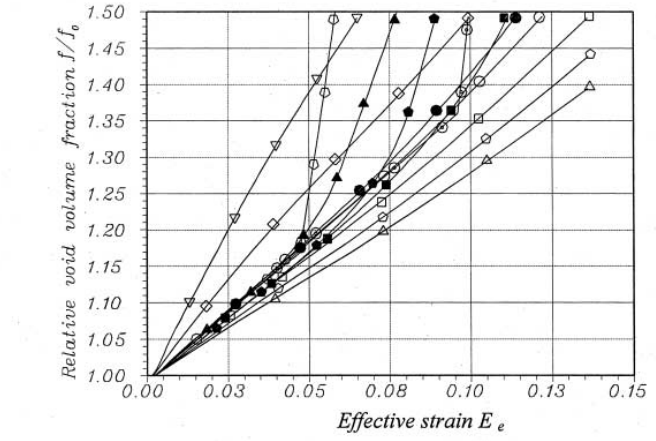

b) in the neck center of notched bar

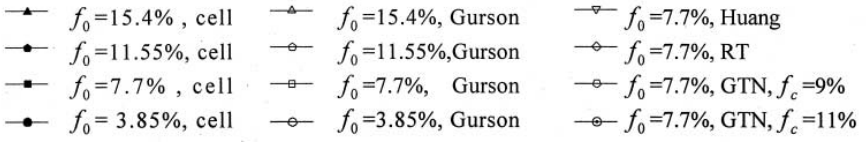

Fig. 7. Void relative growth vs effective strain in neck centres of round and notched bars.

$$f^* = \begin{cases} f & \text{for } f \leqslant f_c \\ f_c + K(f - f_c) & \text{for } f > f_c \text{ with } K = \dfrac{f_u^* - f_c}{f_f - f_c} \end{cases} \tag{10}$$

The parameters f_c and f_f in eqn (10) depend on the damage and fracture of materials, $f_u^* = 1/q_1$. The material exhausts its stress carrying capacity when $f = f_f$.

And the void volume growth in the GTN model or the Gurson model can be found by integrating the following equation

$$\mathrm{d}f = \frac{3}{2} q_1 f^* (1-f) \sin h\left(\frac{3\Sigma_\mathrm{h}}{2\sigma_\mathrm{M}}\right) \frac{\sigma_M}{\Sigma_\mathrm{e}} \mathrm{d}E_\mathrm{e}^\mathrm{p} \tag{11}$$

The RT model (Rice and Tracey, 1969) predicts the void growth in terms of the radius of sphere void

$$\frac{\mathrm{d}r}{r} = 0.283 \exp\left(\frac{3\Sigma_\mathrm{h}}{2\Sigma_\mathrm{e}}\right) \mathrm{d}E_\mathrm{e}^\mathrm{p} \tag{12}$$

The modified RT model (Huang, 1991) can be written as

$$\left.\begin{aligned} \frac{\mathrm{d}r}{r} &= 0.427 \left(\frac{\Sigma_\mathrm{h}}{\Sigma_\mathrm{e}}\right)^{1/4} \exp\left(\frac{3\Sigma_\mathrm{h}}{2\Sigma_\mathrm{e}}\right) \mathrm{d}E_\mathrm{e}^\mathrm{p} \quad \text{for } \frac{\Sigma_\mathrm{h}}{\Sigma_\mathrm{e}} \leqslant 1 \\ \frac{\mathrm{d}r}{r} &= 0.427 \exp\left(\frac{3\Sigma_\mathrm{h}}{2\Sigma_\mathrm{e}}\right) \mathrm{d}E_\mathrm{e}^\mathrm{p} \quad \text{for } \frac{\Sigma_\mathrm{h}}{\Sigma_\mathrm{e}} > 1 \end{aligned}\right\} \tag{13}$$

In eqns (12) and (13), r is the current void radius, Σ_h, Σ_e and E_e^p, are respectively the remote hydrostatic stress, effective stress and effective plastic strain.

For a cell containing a spherical void as defined in Fig. 2, f is defined by eqn (4); approximately

$$\mathrm{d}f \approx \frac{\mathrm{d}V_\mathrm{void}}{V} = 3f\frac{\mathrm{d}r}{r} \tag{14}$$

Substituting $\dfrac{\mathrm{d}r}{r}$ of eqns (12) and (13) into eqn (14), the void volume increase can be described as

$$\mathrm{d}f = 0.849 f \exp\left(\frac{3\Sigma_\mathrm{h}}{2\Sigma_\mathrm{e}}\right) \mathrm{d}E_\mathrm{e}^\mathrm{p} \tag{15}$$

for the RT model, and

$$\left.\begin{aligned} \mathrm{d}f &= 1.281 f \left(\frac{\Sigma_\mathrm{h}}{\Sigma_\mathrm{e}}\right)^{1/4} \exp\left(\frac{3\Sigma_\mathrm{h}}{2\Sigma_\mathrm{e}}\right) \mathrm{d}E_\mathrm{e}^\mathrm{p} \quad \text{for } \frac{\Sigma_\mathrm{h}}{\Sigma_\mathrm{e}} \leqslant 1 \\ \mathrm{d}f &= 1.281 f \exp\left(\frac{3\Sigma_\mathrm{h}}{2\Sigma_\mathrm{e}}\right) \mathrm{d}E_\mathrm{e}^\mathrm{p} \quad \text{for } \frac{\Sigma_\mathrm{h}}{\Sigma_\mathrm{e}} > 1 \end{aligned}\right\} \tag{16}$$

for Huang's modified RT model.

From Fig. 7, comparing these curves drawn from Gurson model, GTN model, RT model and the modified RT model with the present results of the cell model calculation, it can be stated that the descriptions of the void stable growth by the Gurson model and the GTN model agree with those of the cell model calculations. The RT model and its modified model are not as precise as the Gurson model and the GTN model. This may be due to the fact that the RT model ignores the effect of finite volume and in the present case the void size is fairly large compared to the cell. This is very different from the case of a void in an infinite solid.

If one chooses $q_1 = 1.1, q_2 = 1, q_3 = q_1^2$, the void stable growth described by the GTN model can be well fitted so that it is consistent with the cell model calculation result. Furthermore, if set to $f_c = 9\%$, then the GTN model can predict the fracture of round smooth specimen under tension. However, if the GTN model is applied with the parameter $f_f = 9\%$ to describe the fracture of the round notched specimen under tension, the result is slightly more than half that of the test data. If set to $f_c = 11\%$, then the result will be in good agreement with test data. These are also shown in Fig. 7. This result means that the parameter f_c may not be a constant as expected. In the present condition, the higher the stress triaxiality is, the larger the parameter f_c is.

In Fig. 7, it can also be seen that the cell model calculations, excepting the case using the cell with $f = 15.4\%$, do not represent the void expansion in unstable state. The void in the cell does not expand but constricts in the cross section direction, where the stress triaxiality is controlled following the case in the neck center of a round smooth bar. Therefore, the results show that if the average values of f and spacing in principal stress directions in material are used in the calculation, the prediction for the fracture of the material element will be overestimated compared with the actual case. It also means that the damage and fracture in material may first take place in the region where strength is the weakest. The results of such a cell model for which geometric parameters take the average statistical characteristics will not be consistent with the experimental tests.

In Fig. 8, the results are calculated for cells which are different for L_{r0} or for S_{r0}. $L_{r0} \neq 1$ means that the spacing is different in loading direction from that in the across section direction. $S_{r0} \neq 1$ means the hole in the cell is not spherical but ellipsoidal. In this figure it can be found that the influence of non-uniform spacing on the void unstable expansion in a cell is very significant. If $L_{r0} > 1$, for example $L_{r0} = 2$, which means the spacing in the cross section direction is less than that in tension loading direction, the void in such a cell grows in the across section direction when void unstable expansion occurs, under the condition that the stress triaxiality of the cell is controlled as in the neck center of the round smooth specimen under tension. If $S_{r0} > 1$, the ellipsoidal (oblate) void growth in volume is also faster than the average case but the effect is not as significant as that of non-uniform spacing. Here the initial inclusions can not be considered too oblate in geometry for a nodular cast iron material. In Fig. 8, it can also be found that if the factors $L_{r0} < 1$ and $S_{r0} < 1$ are considered, the void growth in volume will be slowed.

It is necessary to point out that when the microscopic fracture takes place in the material element as predicted by using a non-uniform cell, the macroscopic fracture does not take place at the same time. The macroscopic fracture will occur after the coalescence of a number of voids which may depend on the loading conditions and the geometry of the specimens. The process of microscopic fracture should depend on the distribution of void size, shape, spacing and other non-uniform factors which may need to be taken into account for evaluating the fracture criterion of a material from microscopic analysis. The photographs of GGG-40 fracture profile (Dong, 1995) show that the rupture of the material begins at the area where the voids grows in the cross section direction and coalescence, where the voids are larger and closer than those in other places. There are also a number of voids which have not grown to meet each other even after the final fracture. In fact, after the macroscopic crack has been formed by the coalescence of a number of voids, the type of damage will change from coalescence of voids to crack propagation. The latter takes place more easily because it requires much less energy. So the microscopic fractures do not take place at the same step in the material, and not in the same way.

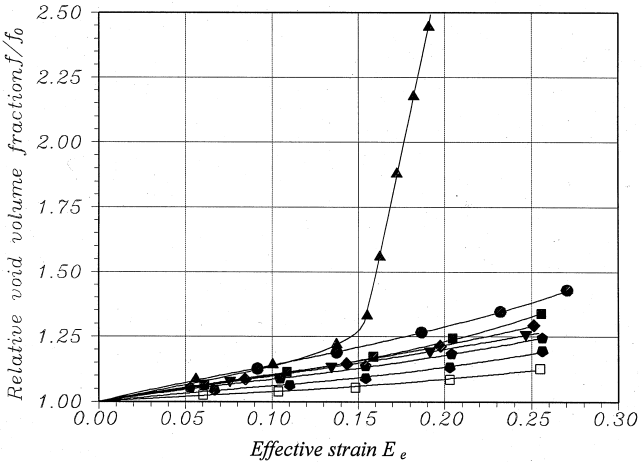

a) in the neck center of round bar

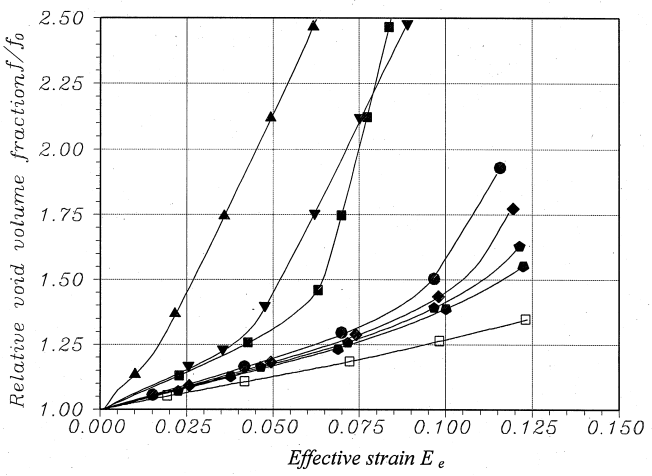

b) in the neck center of notched bar

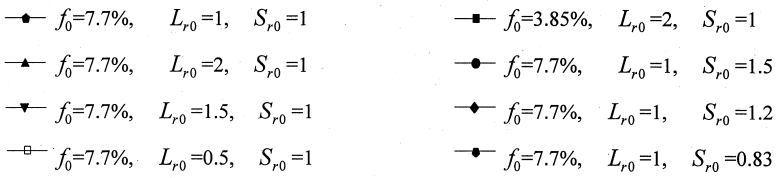

Fig. 8. The relative fraction f/f_0 of the cells in which $L_{r0} \neq 1$ or $S_{r0} \neq 1$.

Figure 9 shows the deformed mesh calculated by using the cell model with the parameters $L_{r0} = 2$, $S_{r0} = 1$ and $f_0 = 7.7\%$ (effective strain $E_e^p = 0.21$), under the condition simulating the material in the neck center of round smooth specimen. For comparison the deformed mesh calculated by using the cell model with parameters $L_{r0} = 1$, $S_{r0} = 1$ and $f_0 = 7.7\%$ (effective strain has reached $E_e^p = 0.43$) under the same conditions is also shown in the same figure. According to

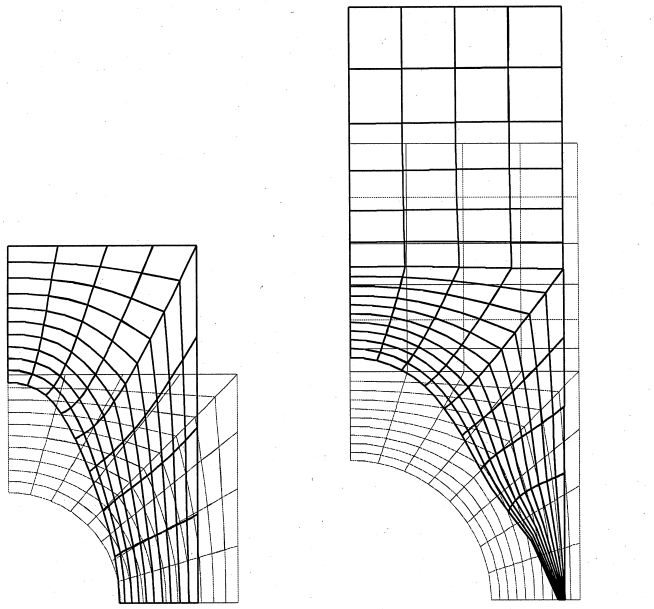

Fig. 9. Deformations of the cell with identical spacing and the cell with non-uniformed spacing (both are of same $f_0 = 7.7\%$).

the figure it may be noted that the influence of void spacing on the void growth, especially on the void unstable growth is very significant. In the case of a cell with identical spacing under low stress triaxiality, a void will grow very fast in the tension direction and constrict in the cross section direction. But in the case the parameter $L_{r0} > 1$, that is, the void spacing in tension direction is larger than that in the cross section direction, the void will grow in the cross section direction after a few percents strain. And the greater the parameter L_{r0}, the smaller the strain for void growth in the cross section direction will be. It is necessary to point out that, according to experiment study, the microscopic failure of GGG-40 is mainly caused by one void causing other voids to intersect with each other. So whether the model can or can not predict the void expanding in the cross section direction is very important in cell model calculations.

Figure 10 shows the curves of void volume fraction vs effective strain for the axisymmetric cell which contains two voids of different size. From this figure, it may be noted that the larger void grows faster than the smaller one for the periodic array of voids in Fig. 3. This result means that if the void size in the material is not uniform, the void expansion in the material either will not be uniform, and the larger voids may grow faster than the smaller ones. This result is very different from that obtained by the cell model with a spherical void in its center and with uniform spacing where the relative growth in volume fraction of the voids of different size is nearly the same (cf Fig. 7). This case is very similar to the case where $L_{r0} = 2$, which means the smaller void in the cell play a role in causing the cell spacing to be non-uniform in the cross section and in tension loading directions. As the radius of the smaller void in the cell approaches zero, the case where $L_{r0} = 2$ can be approximated with the periodic array of voids described in Fig. 3.

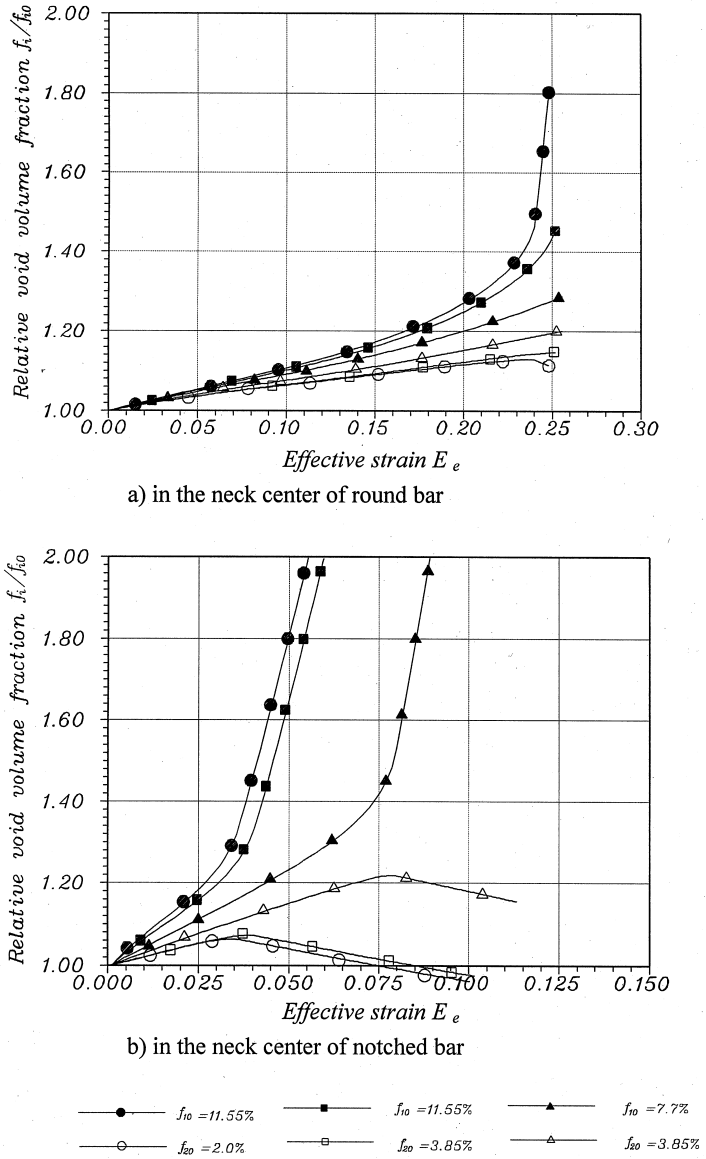

Fig. 10. Evolution of f/f_0 of the cylindrical cell containing two voids with different size; a) in the neck centre of round bar; b) in the neck centre of notched bar.

Figure 11 shows the deformed meshes of the cell model containing an ellipsoidal void $S_{r0} = 1.5$, $L_{r0} = 1$, $f_0 = 7.7\%$, (effective strain $E_e^p = 0.32$), and of the cell model containing two spherical voids of different size $f_{10} = 5.775\%$, $f_{20} = 1\%$, $E_e^p = 0.25$ under the loading condition in the neck center of the round bar. It can be seen that the ellipsoidal void expands in the tension direction and constricts in the cross section direction. In the cell containing two voids, the void growth rates are very different: the larger void has grown in an unstable state, the smaller is still in a stable

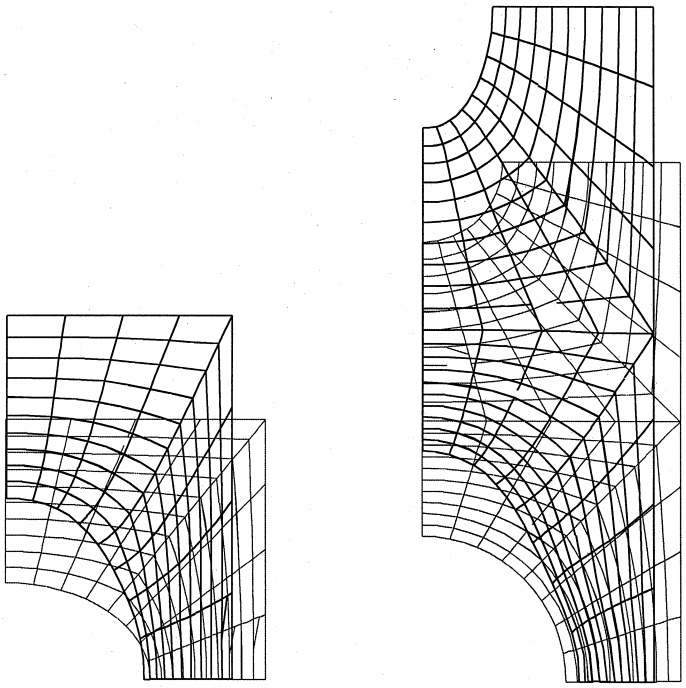

Fig. 11. The deformed meshes of a cell containing an ellipsoidal void and a cell containing two spherical voids with different size.

state. According to the detailed analysis, the area around the smaller void is even unloaded. In fact from Fig. 10 it can be seen that the volume fraction has decreased.

Figure 12 shows the curves of effective stress vs effective strain for different cells. It can be seen that the different geometric cells containing different voids cause the differences in the stress carrying capacity of material elements. It is known that in a real case the microscopic structures of a material are very different in different regions following some statistical distributions of void size, shape and spacing. It can be considered that before the rupture of a specimen takes place the microscopic failure has begun in some places where the void size, shape and spacing may cause the weakness in resistance to fail. The rupture of the specimen made of a material with high void volume fraction like GGG-40 is a complicated microscopic process, which may begin from the intersection of two or several voids, by the voids expanding in the cross section direction, meeting each other, then the intersected voids will speed up the expansion, acting as a crack. When the surface which is formed by the coalescence of the voids reaches a critical value, the specimen will fracture. Because the non-uniform distribution of void size, shape and spacing play a very important role, a cell model seeking to predict the fracture behavior of a material should be established according to these aspects.

The results for 3D cells containing two voids of different size are shown in Fig. 13. This cell has

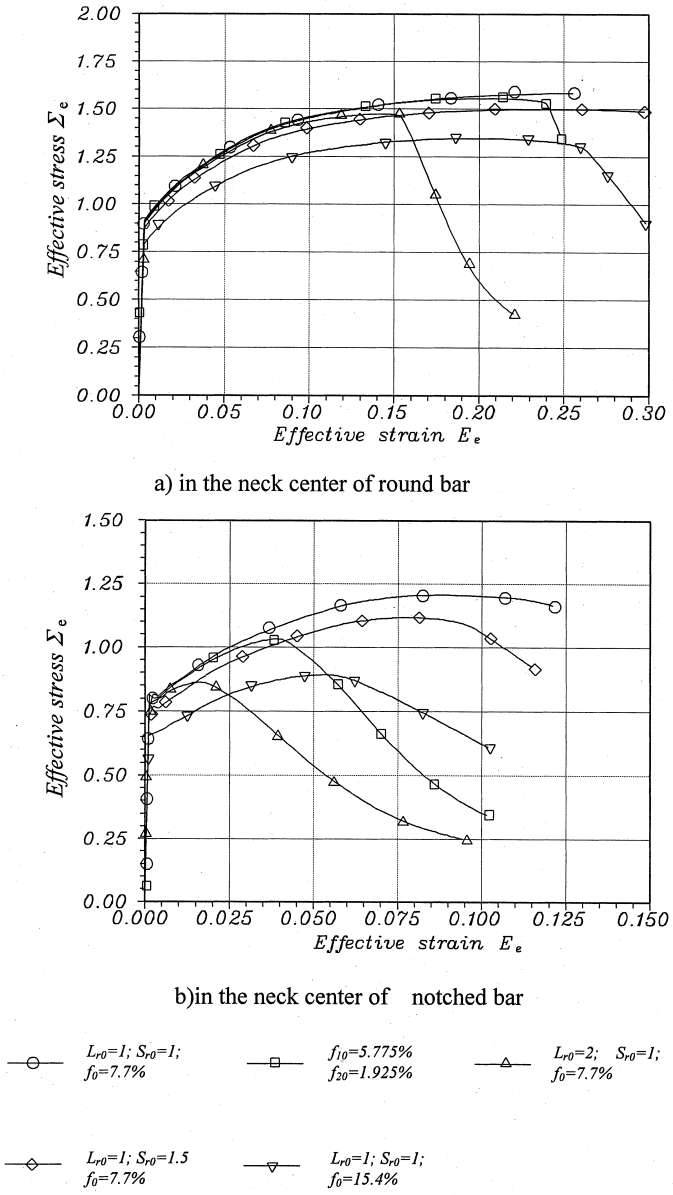

Fig. 12. Effective stress vs effective strain for different cells.

a different periodic array of voids (cf Fig. 4) compared to the case in Fig. 3. It is very interesting to note that the curves by 3D cell calculations are very different from those of the axisymmetric cell described in Fig. 3. Figure 13 shows that the interaction between two voids is much less than that calculated by using a cylindrical cell containing two voids of different size (cf Fig. 11). The larger void in the cell grows slightly faster than the smaller one in the same cell, under the loading conditions in the neck center of round smooth specimen. The larger void grows slightly slower

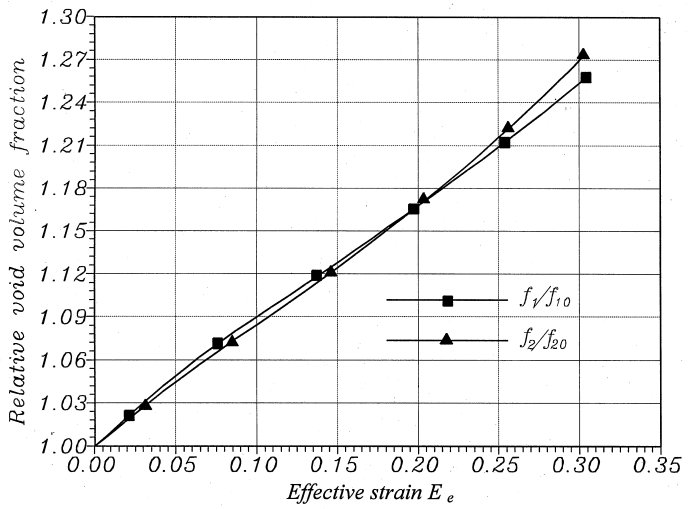

a) in the neck center of round bar

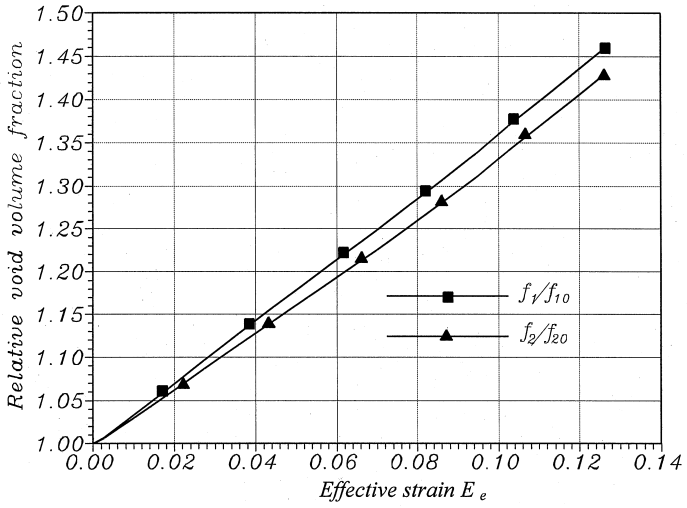

b) in the neck center of notched bar

Fig. 13. The volume growth of the voids with different size ($f_{10} = 4.812\%, f_{20} = 2.888\%$) in the 3D cell.

than the smaller, if the cell has the situation of the neck center of round notched specimen, as shown in the same figure. This result implies that the interaction between two voids of different size depends very much on the periodic pattern used. The interaction between voids can be large or small depending on the distribution of the voids.

It is necessary to point out that no such ideal periodic array of voids can be found in a real material. The array is only an assumption to be used to simplify the analysis and the calculation, so that it can simulate and represent the microscopic process of the evolution of voids in a material

under certain conditions. The results may be very different if different periodic arrays of voids are assumed and modeled by using a corresponding cell model. Considering this, it might be reasonable to take the statistical characteristics of the microstructures into account when constructing the cell model. The new cell probably has different dimensions in the two (2D model) or three (3D model) directions which results in some anisotropic aspect. The 'anisotropic' cell can only be used for the prediction of failures and not the constitutive law modeling. The work under progress consists of introducing the idea of critical volume under consideration and establishing the quantitative procedure to correlate the statistical characteristics of void distribution to the cell dimensions.

5. Conclusions

In the present paper, the microscopic ductile fracture of smooth and notched specimens under tension has been investigated by using FEM calculations. The material is a nodular cast iron with high graphite inclusion, volume fraction 7.7%, and can be considered as a porous medium containing voids of the same size. In order to investigate the failure mechanism of the unstable growth and coalescence of voids the different axisymmetric cell models containing one void or two voids with different geometry and a 3D cell model containing two voids of different size have been used. The effect of size, spacing and array of voids on the void growth law has been taken into account. The results have been compared with the Gurson, GTN and RT models.

According to the results, the following conclusions can be drawn

(1) The cell model containing two voids of different size can produce very different results for void growth in volume and for the interaction of voids; it depends on the pattern of the periodic array of voids used. The interaction is larger for an axisymmetric cell model than for 3D cell model employed in the present paper. A larger void grows faster than a smaller one in the case of a round smooth specimen, but slower in the case of a round notched specimen.
(2) Gurson Model and the GTN model can describe the void growth for a material with high initial void volume fraction until unstable state. However, the RT model and the modified RT model can not give reasonable results.
(3) The parameter f_c to predict the void coalescence used in the GTN model is sensitive to the stress triaxiality. The higher the stress triaxiality is, the larger the parameter f_c is.
(4) When considering non-uniform spacing between voids or the non-uniform initial void volume fraction, the unstable growth of voids consistent with the test data, can be obtained by cell model calculation; and when taking uniform void size and uniform spacing, the result is much greater than the experimental data.
(5) The statistical characteristics of void distribution patterns should be incorporated in the cell model construction so as to correctly predict the final failure strain. This 'anisotropic' cell can only be used for failure prediction and not for constitutive law modeling.

Acknowledgements

The present research was initiated with the support from National Natural Science Foundation of China and completed during the stay as invited professor of one of the authors (KSZ) at Ecole

Centrale Paris, which is highly acknowledged. The authors are grateful for the assistance rendered by their colleagues and their discussions with Prof. Ph. Bompard and Dr C. Berdin.

References

Brocks, W., Hao, S., Steglich, D., 1996. Micromechanical modeling of the damage and toughness behavior of nodular cast iron materials. J. de Physique IV 6 C6, 43–52.

Brocks, W., Sun, D.-Z., Honig, A., 1995. Verification of the transferability of micromechanical parameters of cell model calculations with visco-plastic materials. Int. J. Plasticity 11, 971–998.

Dong, M.-J., 1995. Ph. D. thesis of Ecole Centrale Paris.

Dong, M.-J., Berdin, C., Beranger, A. S., Prioul, C., 1996. Damage effect in the fracture toughness of nodular cast iron. J. de Physique IV 6 C6, 65–74.

Gurson, A. L., 1977. Continuum theories of ductile rupture by void nucleation and growth: Part 1—Yield criteria and flow rules for porous ductile media. J. Eng. Mater. Tech. 99, 2–15.

Huang, Y., 1991. Accurate dilation rates for spherical voids in triaxial fields. J. Appl. Mech. 58, 1084–1086.

Koplik, J., Needleman, A., 1988. Void growth and coalescence in porous plastic solids. Int. J. Solid Struct. 24, 835–853.

Kuna, M., Sun, D.-Z., 1996. Analyses of void growth and coalescence in cast iron by cell models. J. de Physique IV 6 C6, 113–122.

Rice, J. R., Tracey, D. M., 1969. On the ductile enlargement of voids in triaxial stress fields. Int. J. Mech. Phys. Solids 17, 201–217.

Tvergaard, V., 1982. Ductile fracture by cavity nucleation between larger voids. J. Mech. Phys. Solids 30, 265–286.

Tvergaard, V., 1996. Effect of void size difference on growth and cavitation instabilities. J. Mech. Phys. Solids 44(8), 1237–1253.

Tvergaard, V., Needleman, A., 1984. Analysis of the cup-cone fracture in a round tensile bar. Acta Metall. 32, 157–169.

Worswick, M. J., Pick, R. J., 1990. Void growth and constitutive softening in a periodically voided solid. J. Mech. Phys. Solids 38(5), 601–625.

Zhang, K. S., Zheng, C. Q., 1997. 3D Analysis of spherical void contained cell under different triaxial stress state. New Progress of Solid Mechanics. Tsinghua University Press.